# Numerically Efficient Algorithm for Compact Microwave Device Optimization with Flexible Sensitivity Updating Scheme

Short title: **Fast Microwave Design Optimization**

Anna Pietrenko-Dabrowska[1] and Slawomir Koziel[2]

[1] Faculty of Electronics, Telecommunications and Informatics, Gdansk University of Technology, 80-233 Gdansk, Poland, **Corresponding author:** anna.dabrowska@pg.edu.pl

[2] Engineering Optimization & Modeling Center, Reykjavik University, 101 Reykjavik, Iceland, koziel@ru.is,

**Anna Pietrenko-Dabrowska** received the M.Sc. and Ph.D. degrees in electronic engineering from Gdansk University of Technology, Poland, in 1998 and 2007, respectively. Currently, she is an Associate Professor with Gdansk University of Technology, Poland. Her research interests include simulation-driven design, design optimization, control theory, modeling of microwave and antenna structures, numerical analysis.

**Slawomir Koziel** received the M.Sc. and Ph.D. degrees in electronic engineering from Gdansk University of Technology, Poland, in 1995 and 2000, respectively. He also received the M.Sc. degrees in theoretical physics and in mathematics, in 2000 and 2002, respectively, as well as the PhD in mathematics in 2003, from the University of Gdansk, Poland. He is currently a Professor with the School of Science and Engineering, Reykjavik University, Iceland. His research interests include CAD and modeling of microwave and antenna structures, simulation-driven design, surrogate-based optimization, space mapping, circuit theory, analog signal processing, evolutionary computation and numerical analysis.

**Keywords:** Design closure, microwave optimization, EM-driven design, gradient search, trust-region framework, Broyden update.

**Abstract**

An efficient trust-region algorithm with flexible sensitivity updating management scheme for electromagnetic (EM)-driven design optimization of compact microwave components is proposed. During the optimization process, updating of selected columns of the circuit response Jacobian is performed using a rank-one Broyden formula (BF) replacing finite differentiation (FD). The FD update is omitted for directions sufficiently well aligned with the recent design relocation. As the algorithm converges, the alignment threshold is gradually reduced so that the condition for using BF becomes less stringent. This allows for further reduction of the number of EM simulations involved in the optimization process. The presented flexible Jacobian update scheme allows for considerable reduction of the computational cost with only slight degradation of the design quality. Robustness of the presented algorithm is validated through multiple optimization runs from random initial designs. The verification experiments are conducted for a range of microwave components, including a compact microstrip coupler as well as a three-section CMRC-based impedance transformer. The effects of the alignment threshold value on the computational efficiency of the algorithm and the design quality are investigated. Significant savings reaching fifty percent as compared to the reference algorithm are demonstrated.

## 1. Introduction

Nowadays, full-wave electromagnetic (EM) analysis is a necessity in the design closure of microwave components and devices [1]. This especially applies to miniaturized structures: due to significant cross-coupling effects present in the densely arranged layouts, simplified representations (e.g., equivalent networks) either cannot be relied on or simply do not exist [2]. The examples of such structures include compact microstrip couplers [3], power dividers [4], impedance transformers [5], and filters [6]. The lack of dependable yet simple equivalent representations affects, to an even greater extent, design optimization of microwave components implemented with the use of slow-

wave structures [7], such as compact microwave resonant cells (CMRCs) [5]. Furthermore, an increased number of geometry parameters describing CMRC-based or other miniaturized circuits (as compared to their conventional transmission-line-based realizations), may result in unmanageable computational overhead of the optimization process.

The reduction of the number of time-consuming EM analyses, otherwise indispensable to ensure reliable evaluation of the circuit under design, can be achieved—among others—by using adjoint sensitivities [8]. Unfortunately, the major setback for the usage of this technology is a limited support for it in commercial EM simulation packages. An alternative approach, allowing us to optimize geometry parameters of multivariate models with a limited number of electromagnetic simulations, are parametric reduced-order models [9]. In recent years, surrogate-based optimization (SBO) [10], [11], has become a common method of choice to improve computational efficiency of EM-driven design. SBO works by replacing direct optimization of the expensive (high-fidelity) model with the iterative process of tuning a cheaper, yet less accurate, surrogate model. With the majority of operations cast onto the surrogate, the optimized design can be identified at the lower computational cost. Here, the principal use of the surrogate is to act as a prediction tool guiding the process towards a better design. The SBO procedures are iterative ones with the recently acquired high-fidelity data employed to improve the model. Computational speedup yielded by SBO is founded on the following two conditions: the surrogate delivers sufficiently accurate description of the structure at hand, and, at the same time, it is significantly faster than the high-fidelity model. SBO methods comprise, among others, the well-recognized space-mapping (SM) [12] as well as various response

correction techniques (manifold mapping [13], [14], shape preserving response prediction [15], adaptive response scaling [16]). Another SBO technique is feature-based optimization (FBO) [17], [18] in which the original problem is reformulated in terms of so-called characteristic points. For structures with well-defined response structure (e.g., multi-band antennas), FBO "flattens" the functional landscape to be handled, thus leading to lower computational expenses.

The surrogate models are constructed either from sampled high-fidelity EM data (data-driven or approximation models) or they are physics-based. The physics-based models (e.g., corrected equivalent networks commonly used by SM [12]) are more problem-dependent and less general, however, they are less affected by the curse of dimensionality. The effectiveness of SBO physics-based methods is strongly determined by the underlying low-fidelity model. The equivalent network representations of miniaturized microwave components frequently provide insufficient accuracy, thus their usage in conjunction with the SBO techniques may be of limited value. On the other hand, the multipurpose, data-driven models, involving kriging interpolation [19] or neural networks [20], [21], are limited to rather low-dimensional cases [19]. This is because the number of required training data samples grows quickly with the number of the model parameters. Consequently, the computational cost of developing surrogate model can surpass the cost of direct optimization of the fine model.

No matter what kind of optimization technique is utilized, either direct or surrogate-assisted, the key issue is to lessen the total computational overhead. Here, a numerically efficient trust-region algorithm with flexible sensitivity updating management scheme is introduced, that allows for achieving a significant computational

speedup. The savings come from omitting a portion of finite differentiation calculations of the circuit response Jacobian. The flexible management scheme is guided by both the alignment between the recent design relocation direction and the coordinate system axes, as well as by the algorithm convergence indicators. For the selected columns of the Jacobian, corresponding to the model parameters for which the alignment is satisfactory (depending on a user-defined threshold), the Jacobian update is performed using a rank-one Broyden formula. With the algorithm converging, the alignment acceptance threshold is adaptively adjusted, and therefore the condition for using the BF relaxes. That leads to further reduction of the number of EM simulations needed by the optimization algorithm.

The proposed technique has been validated at length for two compact CMRC-based structures (a rat-race coupler and an impedance matching transformer). The obtained computational savings as compared to the reference algorithm are substantial. In the future work, the presented algorithm will be employed to accelerate SBO procedures involving variable-fidelity EM models.

## 2. Efficient Optimization with Flexible Sensitivity Updating Scheme

In this section, we formulate the microwave device design problem as an optimization task. In addition, we provide the outline of the conventional trust-region procedure utilized as a reference. Then, the proposed algorithm adopting a flexible sensitivity updating scheme is described in detail. Comprehensive numerical validation involving a range of compact microwave components is provided in Section 3.

### 2.1. Design Closure as an Optimization Task

In this paper, we consider a design closure problem, in which geometry parameter values of a microwave structure at hand are adjusted in order to improve performance

figures of interest. The task is formulated as a nonlinear minimization problem of the form [1]

$$\boldsymbol{x}^* = \arg\min_{\boldsymbol{x}} U(\boldsymbol{R}(\boldsymbol{x})) \tag{1}$$

where $U$ is a nonlinear objective function, $\boldsymbol{R}(\boldsymbol{x})$ represents a response of the EM simulation model of the structure under design, and $\boldsymbol{x}$ denotes a vector of adjustable parameters. A particular definition of the objective function $U$ is determined by both the type of the circuit and design specifications imposed. Let us consider impedance transformers. In that case, a typical objective is to reduce the return loss within the frequency range of interest $F$ which can be formally expressed by defining $U$ as

$$U(\boldsymbol{R}(\boldsymbol{x})) = \max\{f \in F : |S_{11}(\boldsymbol{x}, f)|\} \tag{2}$$

where $|S_{11}(\boldsymbol{x},f)|$ stands for the reflection (here, its dependence on the frequency $f$ and on the geometry parameter vector $\boldsymbol{x}$ is explicitly shown). Another example are microwave couplers, where the performance figures may take different forms, e.g., maximization of the bandwidth $B$ (often with an additional requirement of being symmetric with respect to the operating frequency $f_0$). The optimization problem of a microwave coupler may also be aimed at obtaining the required (equal or non-equal) power split at $f_0$, defined as $d_S = |S_{21}| - |S_{31}|$. Other requirements may be imposed as well, such as allocation of the matching and the isolation characteristics minima close to $f_0$. In the case of multiple objectives, it is a typical practice to select a primary one and cast others into constraints, often handled implicitly, e.g., using penalty functions. With this approach, the objective function may be defined as

$$U(\boldsymbol{R}(\boldsymbol{x})) = -B(\boldsymbol{x}) + \beta_1 d_S(\boldsymbol{x})^2 + \beta_2 (f_{\min.S_{11}}(\boldsymbol{x}) - f_0)^2 + \beta_3 (f_{\min.S_{41}}(\boldsymbol{x}) - f_0)^2 \tag{3}$$

where the frequencies $f_{\min.S11}$ and $f_{\min.S41}$ correspond to the minima of $|S_{11}|$ and $|S_{41}|$, respectively, whereas $\beta_j$, $j$ = 1, 2, 3, denote penalty coefficients. The formulation (3) is a convenient way of handling computationally expensive constraints, commonly occurring in the optimization of EM simulation models [2], [7].

### 2.2. Reference Trust-Region Algorithm

Below, a brief description of a conventional trust-region (TR) gradient search algorithm [22] is given. The TR algorithm allows for a convenient solving of (1) with the objective function and the constraints evaluated through EM analysis. The procedure is iterative and delivers a series of designs $\boldsymbol{x}^{(i)}$, $i$ = 0, 1, …, representing approximations to the optimum solution $\boldsymbol{x}^*$

$$\boldsymbol{x}^{(i+1)} = \arg \min_{\boldsymbol{x};\, -\boldsymbol{\delta}^{(i)} \le \boldsymbol{x}-\boldsymbol{x}^{(i)} \le \boldsymbol{\delta}^{(i)}} U(\boldsymbol{L}^{(i)}(\boldsymbol{x})) \tag{4}$$

where $\boldsymbol{L}^{(i)}(\boldsymbol{x}) = \boldsymbol{R}(\boldsymbol{x}^{(i)}) + \boldsymbol{J}_{\boldsymbol{R}}(\boldsymbol{x}^{(i)})\cdot(\boldsymbol{x} - \boldsymbol{x}^{(i)})$ is a first-order Taylor expansion of $\boldsymbol{R}$ at $\boldsymbol{x}^{(i)}$. Establishing $\boldsymbol{L}^{(i)}$ requires performing calculation of the Jacobian $\boldsymbol{J}_{\boldsymbol{R}}$ through finite differentiation, which involves additional $n$ EM simulations during each algorithm iteration (where $n$ denotes the number of optimizable parameters).

The conventional TR algorithm uses an Euclidean, ball-type search region $\|\boldsymbol{x} - \boldsymbol{x}^{(i)}\| \le \delta^{(i)}$. Here, a different approach is adopted, in which a hypercube-like search region is employed and the inequalities $-\boldsymbol{\delta}^{(i)} \le \boldsymbol{x} - \boldsymbol{x}^{(i)} \le \boldsymbol{\delta}^{(i)}$ of (3) are understood as component-wise. The rationale behind this approach is to accommodate various ranges of the geometry parameters, which may vary from fractions of millimeters (gaps) to tens of millimeters (longitudinal values).

### 2.3. Proposed Trust-Region Optimization Algorithm with Flexible Updating Scheme

In this section, a computationally efficient TR algorithm with flexible sensitivity updating management scheme is depicted. The key concept is a conscientious selection of the columns of the circuit response Jacobian $\boldsymbol{J_R}$, which are to be calculated using an updating formula instead of the finite differentiation. In this paper, a rank-one Broyden update formula is adopted [23], [24]

$$\boldsymbol{J_R}^{(i+1)} = \boldsymbol{J_R}^{(i)} + \frac{\left(\boldsymbol{f}^{(i+1)} - \boldsymbol{J_R}^{(i)} \cdot \boldsymbol{h}^{(i+1)}\right) \cdot \boldsymbol{h}^{(i+1)T}}{\boldsymbol{h}^{(i+1)T} \boldsymbol{h}^{(i+1)}}, \qquad i = 0, 1, \ldots \tag{5}$$

In (5), the following notation is used: $\boldsymbol{f}^{(i+1)} = \boldsymbol{R}(\boldsymbol{x}^{(i+1)}) - \boldsymbol{R}(\boldsymbol{x}^{(i)})$, and $\boldsymbol{h}^{(i+1)} = \boldsymbol{x}^{(i+1)} - \boldsymbol{x}^{(i)}$. It should be underlined that the information about the system sensitivity, contained in the Jacobian estimate $\boldsymbol{J_R}^{(i)}$, calculated upon $i$th iteration, is only pertinent to an $i$-dimensional subspace spanned by the vectors $\boldsymbol{h}^{(1)}$, $\boldsymbol{h}^{(2)}$, …, $\boldsymbol{h}^{(i)}$. Therefore, at least $n$ iterations are necessary to estimate the Jacobian in all $n$ directions. For this reason, poor results are typically obtained with the Jacobian calculated with the sole usage of the BF update formula (5), especially for higher-dimensional spaces (see the results of Section 3).

In our approach, this issue is dealt with using a flexible, both selective and adaptive, sensitivity updating scheme. The Jacobian $\boldsymbol{J_R}$, utilized in the optimization course, is merged from the columns evaluated through FD as well as BF. Selection of the variables for which the Broyden formula is applied, based on the alignment between the most recent design relocation and the coordinate system axes. Furthermore, the selection criterion is adaptively adjusted as the algorithm converges, with the measure of the latter being the TR region size. The flow diagram of the proposed algorithm is shown in Fig. 1.

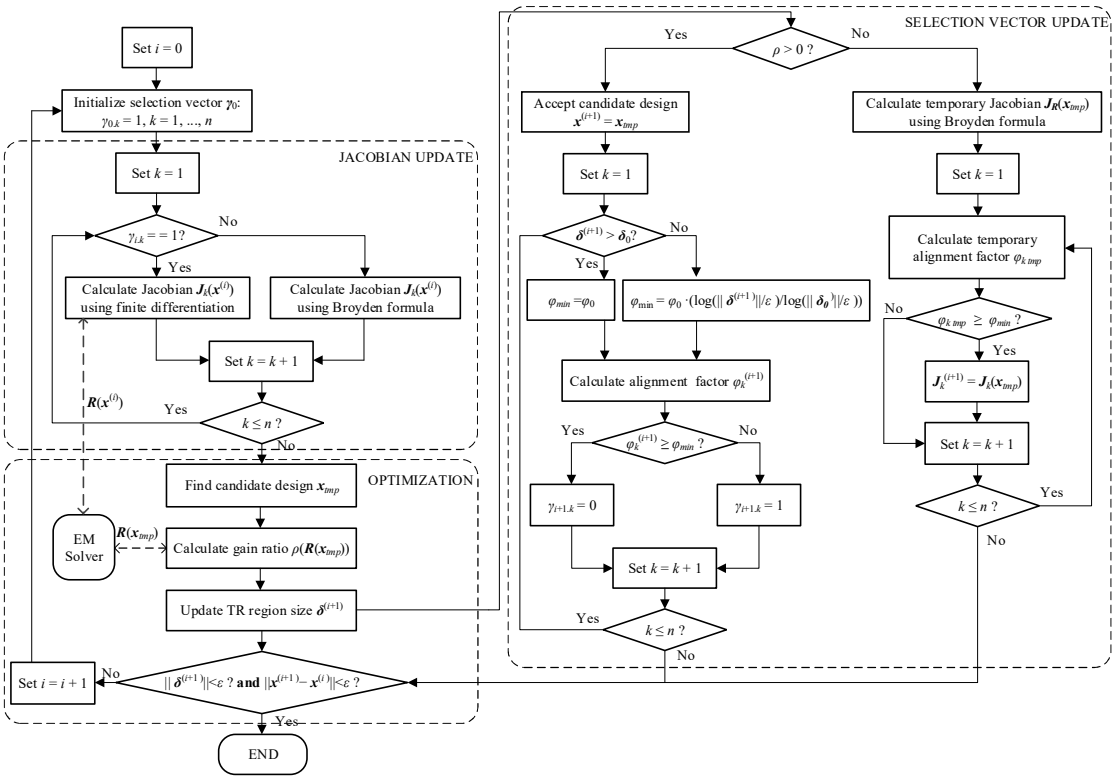


Fig. 1. Flow diagram of the proposed algorithm using flexible sensitivity updating scheme; the following notation is used: $\boldsymbol{\delta}^{(i+1)}$ – TR region size in the ($i$+1)th iteration, $\boldsymbol{\delta}_0$ – TR region size threshold value (below which the alignment threshold $\varphi_{\min}$ starts to decrease); $\varepsilon$ – algorithm termination threshold; $\boldsymbol{\gamma}_i$ – binary selection vector (governing the choice between FD and BF in the $i$th iteration); $\varphi_{\min}$ – alignment acceptance threshold ($\varphi_0$ being its initial value); $\varphi_k^{(i+1)}$ – alignment factors for the ($i$+1)th iteration and the $k$th parameter, $k = 1, \ldots, n$.

The top-left panel of Fig. 1 depicts the Jacobian updating procedure. Let us denote by $\boldsymbol{J}_k = \partial \boldsymbol{R}/\partial x_k$ the $k$th column of $\boldsymbol{J}_\boldsymbol{R}$ (comprising the system response $\boldsymbol{R}$ sensitivities w.r.t. the $k$th parameter). In addition, $\boldsymbol{\gamma}_i$ refers to an $n$-element binary selection vector, that governs the choice between FD and BF in the current ($i$th) iteration: if its $k$th element $\gamma_{i.k}$ equals 1, $k = 1, \ldots, n$, the respective Jacobian column $\boldsymbol{J}_k$ is calculated using FD, if it equals 0 – BF is used instead. The algorithm initializes with all entries of the initial selection vector $\boldsymbol{\gamma}_0$ set to 1, which implies that the initial estimate of the Jacobian $\boldsymbol{J}_\boldsymbol{R}^{(0)}$ is obtained solely with FD.

In the $i$th iteration, after the Jacobian update is completed, the actual optimization procedure is carried out (see the bottom-left panel of Fig. 1). First, (4) is solved and the candidate design $\boldsymbol{x}_{tmp}$ is identified. Then, a gain ratio $\rho = (U(\boldsymbol{R}(\boldsymbol{x}_{tmp}) - U(\boldsymbol{R}(\boldsymbol{x}^{(i)})/(\boldsymbol{L}^{(i)}(\boldsymbol{x}_{tmp}) - \boldsymbol{L}^{(i)}(\boldsymbol{x}^{(i)}))$ is calculated, and the TR region size $\boldsymbol{\delta}^{(i+1)}$ for the next $(i+1)$th iteration is adjusted. Unless the termination criterion is satisfied, i.e., $\|\boldsymbol{\delta}^{(i+1)}\| < \varepsilon$ and $\|\boldsymbol{h}^{(i+1)}\| < \varepsilon$, where $\varepsilon$ is an algorithm termination threshold (here, $\varepsilon = 10^{-3}$), the selection vector for the next iteration is assessed using the procedure shown in the right panel of Fig. 1.

If the iteration was successful (the gain ratio $\rho$ is greater than zero), the candidate design is accepted. Next, the values of the alignment factors $\varphi_k^{(i+1)} = |\boldsymbol{h}^{(i+1)T}\boldsymbol{e}^{(k)}|/\|\boldsymbol{h}^{(i+1)}\|$, which control the selection between the FD and the BF, for each parameter $k$, are calculated. Let $\boldsymbol{e}^{(k)}$ denote the standard basis vectors, $\boldsymbol{e}^{(k)} = [0 \ldots 0\ 1\ 0 \ldots 0]^T$ (1 on the $k$th position). The factors $\varphi_k^{(i+1)}$ serve as a measure of the alignment between the current design relocation $\boldsymbol{h}^{(i+1)}$ and the respective basis vectors $\boldsymbol{e}^{(k)}$. The values of $\varphi_k^{(i+1)}$ range from 0 to 1: $\varphi_k^{(i+1)} = 0$ if the vectors $\boldsymbol{h}^{(i+1)}$ and $\boldsymbol{e}^{(k)}$ are orthogonal, whereas $\varphi_k^{(i+1)} = 1$ if the vectors are co-linear. If the alignment $\varphi_k^{(i+1)}$ is better than a user-defined alignment acceptance threshold $\varphi_{\min}$, the corresponding selection factor $\gamma_{i+1.k}$ is set to 0 (BF), otherwise $\gamma_{i+1.k} = 1$ (FD). The larger the threshold $\varphi_{\min}$, the stricter the condition for using BF becomes, leading to lowering potential computational savings and supposedly a better design quality. On the other hand, lowering $\varphi_{\min}$ may accelerate the optimization process, however, possibly, accompanied by a slight degradation of the design quality.

In this paper, an adaptive algorithm is proposed, in which the alignment threshold value $\varphi_{\min}$ is a function of the TR region size $\|\boldsymbol{\delta}^{(i+1)}\|$ as shown below

$$\varphi_{\min} = \varphi_0 \cdot \frac{\log\left(\left\|\boldsymbol{\delta}^{(i+1)}\right\| / \varepsilon\right)}{\log\left(\left\|\boldsymbol{\delta}_0\right\| / \varepsilon\right)} \tag{6}$$

Here, $\varepsilon$ is the algorithm termination threshold (for convergence in argument), whereas $\|\boldsymbol{\delta}_0\|$ is a user-defined value of the TR region size, below which the threshold value $\varphi_{\min}$ starts to decrease (here, $\|\boldsymbol{\delta}_0\| = 0.01$). Therefore, the acceptance threshold $\varphi_{\min}$ maintains its initial value $\varphi_0$ until $\|\boldsymbol{\delta}^{(i+1)}\|$ gets below $\|\boldsymbol{\delta}_0\|$. Beyond that value, $\varphi_{\min}$ is gradually reduced and the alignment condition relaxes, reaching zero when approaching convergence. As a consequence, BF is used more frequently. Thus, utilization of (6) allows for additional speedup when compared to the fixed acceptance threshold. Reduction of the acceptance threshold is justified by the fact that, as the algorithm converges, the design relocation between subsequent iterations decreases, hence, the response gradients change less significantly.

In the right panel of Fig. 1, the case of the rejected iteration is also presented. The proposed algorithm exploits the fact that the information comprised in the rejected design can still contribute to a sensitivity estimation enhancement [23]. Thus, the temporary Jacobian $\boldsymbol{J_R}(\boldsymbol{x}_{tmp})$ is calculated using (5) (with $\boldsymbol{x}_{tmp}$ inserted instead of $\boldsymbol{x}^{(i+1)}$), and the temporary alignment factors $\varphi_k{}^i{}_{tmp}$ are calculated. For each parameter $k$, if $\varphi_k{}^i{}_{tmp} \geq \varphi_{min}$, the respective column of the temporary Jacobian $\boldsymbol{J}_k(\boldsymbol{x}_{tmp})$ supersedes the Jacobian column $\boldsymbol{J}_k$, calculated in the previous iteration.

## 3. Case Study and Results

The proposed procedure has been verified using two compact microwave structures implemented on Taconic RF-35 substrate ($\varepsilon_r = 3.5$, $h = 0.762$ mm, tan $\delta = 0.018$). The first structure is an equal-split rat-race coupler (RRC) [25] shown in Fig. 2(a) composed of

compact microstrip resonant cells (CMRCs). The RRC geometry is described by the following parameters: $\boldsymbol{x} = [l_1\ l_2\ l_3\ d\ w\ w_1]^T$, along with $d_1 = d + |w - w_1|$ (a relative variable), as well as fixed dimensions: $d = 1.0$, $w_0 = 1.7$, $l_0 = 15$ (all in mm). The coupler's operating frequency is $f_0 = 1$ GHz (at which the coupler is intended to feature equal power split and good matching and isolation). The second device considered is the 50-to-100 Ohm impedance matching transformer [26] shown in Fig. 2(c), in which the CMRC shown in Fig. 2(b) is incorporated. The parameters of the transformer are $\boldsymbol{x} = [l_{1.1}\ l_{1.2}\ w_{1.1}\ w_{1.2}\ w_{1.0}\ l_{2.1}\ l_{2.2}\ w_{2.1}\ w_{2.2}\ w_{2.0}\ l_{3.1}\ l_{3.2}\ w_{3.1}\ w_{3.2}\ w_{3.0}]^T$. In the RRC case, the design objective is to maximize the symmetric bandwidth at –20 dB level around $f_0$. Whereas for the transformer, minimization of the reflection coefficient within the frequency range from 1.5 GHz to 4.5 GHz is performed.

Table I Performance Statistics of the Proposed Algorithm

| Algorithm | | Compact RRC | | | | Three-section transformer | | | |
|---|---|---|---|---|---|---|---|---|---|
| | | Cost[1] | Cost savings[2] [%] | $B$[3] [GHz] | STD ($B$)[4] [GHz] | Cost[1] | Cost savings[2] [%] | max $\lvert S_{11}\rvert$[5] [dB] | STD (max $\lvert S_{11}\rvert$)[6] [dB] |
| Reference | | 43.0 | – | 0.27 | 0.01 | 160 | – | –22.0 | 0.5 |
| Threshold value $\varphi_0$ | 0[$] | 15.9 | 63.0 | 0.18 | 0.11 | 76.6 | 52.1 | –21.1 | 1.1 |
| | 0.025 | 13.4 | 59.5 | 0.21 | 0.06 | 79.2 | 50.0 | –21.3 | 0.9 |
| | 0.05 | 28.9 | 32.8 | 0.25 | 0.04 | 83.9 | 47.6 | –21.3 | 0.8 |
| | 0.1 | 27.0 | 37.2 | 0.24 | 0.05 | 101.0 | 36.9 | –21.5 | 0.6 |
| | 0.2 | 42.6 | 0.9 | 0.24 | 0.05 | 132.6 | 17.1 | –21.8 | 0.6 |
| | 0.3 | 41.3 | 4.0 | 0.23 | 0.06 | 124.3 | 22.3 | –21.6 | 0.8 |
| | 0.4 | 35.9 | 16.5 | 0.23 | 0.08 | 144.5 | 9.7 | –21.7 | 0.7 |

[1] Number of EM simulations averaged over 10 algorithm runs (random initial points);
[2] Percentage-wise cost savings w.r.t. the reference algorithm;
[3] Objective function values for the compact RRC (bandwidth $B$ in GHz);
[4] Standard deviation of $B$ in dB across 10 algorithm runs;
[5] Objective function values for the three-section transformer (maximum in-band reflection $S_{11}$ in dB);
[6] Standard deviation of $S_{11}$ in dB across 10 algorithm runs;
[$] Broyden-only Jacobian updates meaning no FD used whatsoever.

The following initial values of the alignment threshold were used for both devices $\varphi_0$ = 0, 0.025, 0.05, 0.1, 0.2, 0.3, and 0.4. The results obtained with the proposed algorithm, as well as the conventional TR procedure (used as a reference) are presented in Table I. The statistical data on the algorithm performance was collected by executing ten optimization runs using random start points. Figure 3 shows the initial and optimized responses for the selected algorithm runs.

The results of Table I confirm our presumptions that smaller values of the acceptance threshold $\varphi_0$, associated with less stringent conditions for replacing FD with BF, deliver considerably higher computational cost savings. At the same time, decreasing $\varphi_0$ corresponds with the improvement of the design quality. Hence, the threshold value can be used to control the trade-offs between the computational speedup and the design quality. For the RRC, the boundary threshold value, which ensures acceptable solution quality accompanied by substantial cost savings (around 29%), is $\varphi_0$ = 0.05. For the CMRC-based transformer, the higher threshold value is necessary i.e., $\varphi_0$ = 0.1 for which both the satisfactory design quality is obtained (degradation w.r.t. reference algorithm as low as 0.5 dB) and significant computational speedup (over 36%). The reason for this is a significant difference in the parameter space dimensionality (5 for the RRC versus 15 for the transformer). This suggests making the acceptance threshold dimensionality dependent which will be addressed in the future work. Nevertheless, for both structures substantial savings have been obtained. It should be noted that for the RRC, neither the savings nor the solution quality degradation are monotonic with respect to $\varphi_0$. This, however, is primarily a result of a limited number of optimization runs, leading to a relatively high variance of estimating the statistical moments of the objective function

presented in Table I. It can be suggested that more noticeable cost savings could be attained with the use of the proposed algorithm for more complex structures (described by the number of parameters exceeding 20).

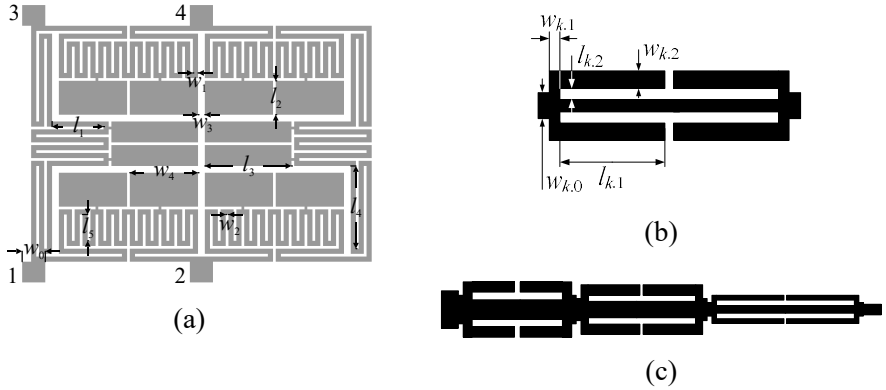


Fig. 2. Microwave structures used for benchmark purposes: (a) microstrip rat-race coupler with slow-wave resonant structures [25], (b) compact microstrip resonant cell being incorporated into a CMRC-based miniaturized three-section impedance transformer (c).

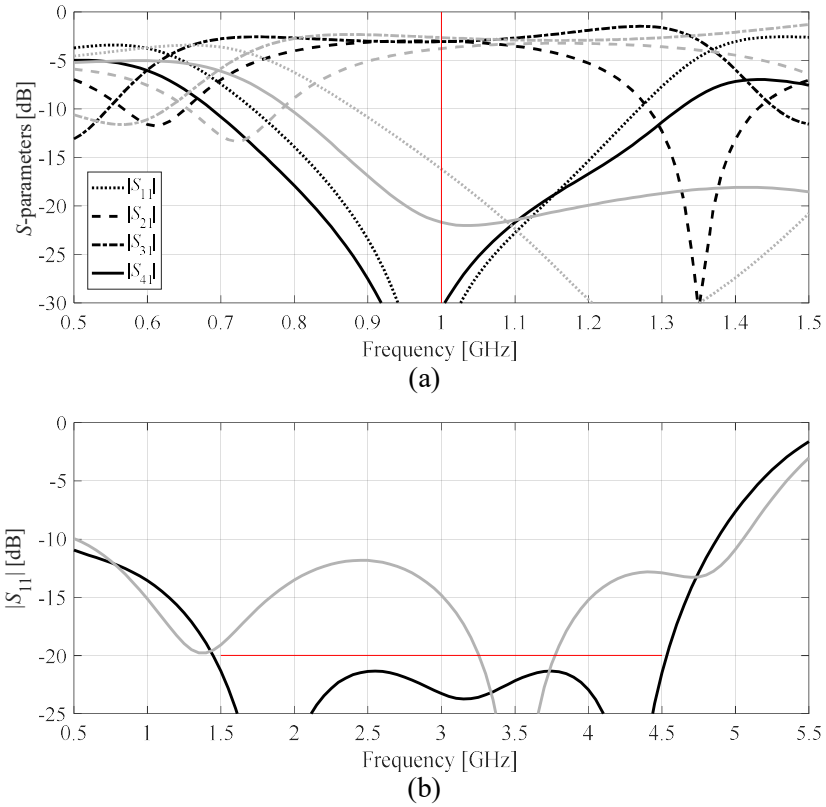


Fig. 3. Characteristics of the considered microwave devices for the representative algorithm runs: (a) compact RRC, (b) three-section impedance matching transformer. The initial and optimized designs are marked gray and black, respectively. The vertical line in (a) indicates the required operating frequency $f_0$, whereas the horizontal line in (b) indicates the required operating bandwidth.

## 4. Conclusion

In the paper, an accelerated gradient-based optimization procedure for EM-driven design of compact microwave components have been presented. Our approach is based on selective Broyden updates of the system response Jacobian, controlled by the alignment of the recent design relocation with the coordinate system basis, as well as the algorithm convergence status. Comprehensive validation demonstrated superiority of the procedure (almost 50 percent speedup) over the conventional TR algorithm used as a reference with minor deterioration of the design quality. The technique can be used for expedited direct EM-based microwave optimization as well as to accelerate variable-fidelity SBO procedures. The latter will be the subject of the future work.

## Acknowledgement

The authors would like to thank Dassault Systemes, France, for making CST Microwave Studio available. This work is partially supported by the Icelandic Centre for Research (RANNIS) Grants 174114051 and 174573052, and by National Science Centre of Poland Grant 2015/17/B/ST6/01857.

## References

[1] Zhang J, Zhang C, Feng F, Zhang W, Ma J, Zhang QJ. Polynomial chaos-based approach to yield-driven EM optimization. *IEEE Trans Microwave Theory Tech.* 2018;66(7):3186-3199.

[2] Koziel S, Kurgan P. Compact cell topology selection for size-reduction-oriented design of microstrip rat-race couplers. *Int J RF Microwave CAE*. 2018;28(5).

[3] Ting HL, Hsu SK, Wu TL. A novel and compact eight-port forward-wave directional coupler with arbitrary coupling level design using four-model control theory. *IEEE Trans Microwave Theory Techn.* 2017;65(2):467-475.

[4] Khan AA, Mandal MK. Miniaturized substrate integrated waveguide (SIW) power dividers. *IEEE Microwave Wireless Comp Lett.* 2016;26(11):888-890.

[5] Koziel S, Bekasiewicz A. Rapid simulation-driven multi-objective design optimization of decomposable compact microwave passives. *IEEE Trans Microwave Theory Tech*. 2016;64(8):2454-2461.

[6] Sheikhi A, Alipour A, Abdipour A. Design of compact wide stopband microstrip low-pass filter using T-shaped resonator. *IEEE Microwave Wireless Comp Lett*. 2017;27(2):111-113.

[7] S. Koziel and P. Kurgan, "Inverse modeling for fast design optimization of small-size rat-race couplers incorporating compact cells," *Int. J. RF & Microwave CAE*, 28(5, 2018.

[8] Y. Zhang, N.K. Nikolova, and M.K. Meshram, "Design optimization of planar structures using self-adjoint sensitivity analysis," *IEEE Trans. Ant. Prop.*, vol 60(6, pp. 3060-3066, 2012.

[9] S. Burgard, O. Farle, P. Loew, and R. Dychij-Edlinger, "Fast shape optimization of microwave devices based on parametric reduced-order models," *IEEE Trans. Magn.*, 50(2, paper No. 7015504, 2014.

[10] J. L. Chávez-Hurtado and J. E. Rayas-Sánchez, "Polynomial-Based Surrogate Modeling of RF and Microwave Circuits in Frequency Domain Exploiting the

Multinomial Theorem," *IEEE Trans. Microwave Theory Tech*, 64(12, pp. 4371-4381, Dec. 2016.

[11] N. Leszczynska, I. Couckuyt, T. Dhaene and M. Mrozowski, "Low-Cost Surrogate Models for Microwave Filters," *IEEE Microwave Wireless Comp Lett*, 26(12, pp. 969-971, Dec. 2016.

[12] J.W. Bandler, Q.S. Cheng, S.A. Dakroury, A.S. Mohamed, M.H. Bakr, K. Madsen, and J. Sondergaard, "Space mapping: the state of the art," *IEEE Trans. Microwave Theory Tech.*, 52(1, pp. 337-361, Jan. 2004.

[13] Y. Su, J. Li, Z. Fan, and R. Chen, "Shaping optimization of double reflector antenna based on manifold mapping," *Int. Applied Comp. Electromagnetic Society Symp. (ACES)*, pp. 1-2, Aug. 1-4, Shuzou, China, 2017.

[14] J. Xu, M. Li, and R. Chen, "Lump-loaded antenna optimization by manifold mapping algorithm with method of moments", *Eng Anal Bound Elem*, 89, pp. 45-49, 2018.

[15] L. Leifsson, and S. Koziel, "Surrogate modeling and optimization using shape-preserving response prediction: a review," *Engineering Optimization*, 48(3, pp. 476-496, 2014.

[16] S. Koziel and A. Bekasiewicz, "Rapid microwave design optimization in frequency domain using adaptive response scaling," *IEEE Trans. Microwave Theory Tech.*, 64(9, pp. 2749-2757, 2016.

[17] S. Koziel, "Fast simulation-driven antenna design using response-feature surrogates," *Int. J. RF & Microwave CAE*, 25(5, pp. 394-402, 2015.

[18] C. Zhang, F. Feng, V. Gongal-Reddy, Q. J. Zhang and J. W. Bandler, "Cognition-driven formulation of space mapping for equal-ripple optimization of microwave filters," *IEEE Trans. Microwave Theory Tech*, 63(7, pp. 2154-2165, July 2015

[19] D.I.L. de Villiers, I. Couckuyt, and T. Dhaene, "Multi-objective optimization of reflector antennas using kriging and probability of improvement," *Int. Symp. Ant. Prop.*, pp. 985-986, San Diego, USA, 2017.

[20] C. Zhang, J. Jin, W. Na, Q.J. Zhang, and M. Yu, "Multivalued neural network inverse modeling and applications to microwave filters," *IEEE Trans. Microwave Theory Tech.*, 66(8, pp. 3781-3797, 2018.

[21] F. Feng, C. Zhang, J. Ma, and Q. Zhang, "Parametric modeling of EM behavior of microwave components using combined neural networks and pole-residue-based transfer functions," *IEEE Trans. Microwave Theory Techn*, 64(1, pp. 60-77, Jan. 2016

[22] A.R. Conn, N.I.M. Gould, and P.L. Toint, *Trust Region Methods*, MPS-SIAM Series on Optimization, 2000.

[23] J. Nocedal, S.J. Wright, *Numerical Optimization*, 2nd edition, Springer, New York, 2006.

[24] C.G. Broyden, "A class of methods for solving nonlinear simultaneous equations," *Math. Comp.*, 19, pp. 577-593, 1965.

[25] S. Koziel, A. Bekasiewicz, and P. Kurgan, "Rapid design and size reduction of microwave couplers using variable-fidelity EM-driven optimization," *Int. J. RF & Microwave CAE*, 26(1, pp. 27-35, Jan. 2016.

[26] S. Koziel, A. Bekasiewicz,. “Rapid simulation-driven multi-objective design optimization of decomposable compact microwave passives,” *IEEE Trans. Microwave Theory and Techn,* 64(8, pp. 2454-2461, 2016.